

Photon bunching and multiphoton interference in parametric down-conversion

Z. Y. Ou

Department of Physics, Indiana University Purdue University at Indianapolis, Indianapolis, Indiana 46202

J.-K. Rhee and L. J. Wang

NEC Research Institute, Incorporated, 4 Independence Way, Princeton, New Jersey 08540

(Received 9 February 1999)

A number of multiphoton interference schemes involving independent fields from parametric down-conversion are analyzed. They include fourth-order (two-photon) interference between two fields from two independent parametric down-conversion processes, interference with two independent single photon Fock states (produced by gated parametric down-conversion), and quantum state teleportation and entanglement swapping. It is shown that the visibility in these interference experiments is related to a quantity that is responsible for the photon bunching effect in one of the fields (signal or idler) from the parametric down-conversion process. Besides the two-photon interference schemes, a four-photon interference scheme is discussed where we consider four-photon partition at a beamsplitter. It is found that probability distribution of the partition is dramatically changed by four-photon interference of six paths and the four-photon effect also depends on the same quantity responsible for photon bunching. We will discuss the difference between two-photon interference and four-photon interference. [S1050-2947(99)05107-0]

PACS number(s): 42.50.-p, 42.65.-k, 42.25.Hz

I. INTRODUCTION

Generation of multiparticle entangled states has attracted much attention ever since Greenberger, Horne, and Zeilinger (GHZ) [1] showed that more dramatic violation of locality by quantum mechanics can be achieved with these states. So far the proposed schemes for the generation of multiparticle entangled states are based on interference between independent fields from parametric down-conversion [2,3]. The idea behind these schemes is the possibility of creation of four-photon GHZ state by accidentally combining two pairs of independent down-converted photons. Interference with independent fields from parametric down-conversion is also applied to quantum information processing, such as quantum state teleportation where two-photon entangled states are used to teleport an arbitrary unknown polarization state [4–7]. In all these applications, high visibility in interference is necessary to make the GHZ argument on nonlocality and to increase the fidelity of the teleported state. Furthermore, interference among independent fields plays a crucial role in the correct outcome in quantum computing [8].

On the one hand, high visibility is easily achievable in quantum interference involving two correlated photons [9]. On the other hand, because of the independent nature of the down-converted fields involved in the interference schemes mentioned above, stationary fields cannot be used unless the bandwidth of the fields is much smaller than that of the detectors [10], or in other words, the coherent length of the down-conversion field must be long enough so that within the detection time period, the phases of the fields are constant. However, such a requirement can be relaxed if nonstationary fields are used. Zukowski *et al.* [11] and Rarity [12] recently showed that if an ultrashort pulse is used for pumping the parametric down-conversion process, the timing provided by the ultrashort pump pulse can overcome the problem of slow detectors. But high visibility in interference

requires that pulse shapes of the down-converted fields overlap in time (temporal mode matching). Because of the intrinsic incoherent nature of the parametric down-conversion process and the dispersion in the nonlinear medium, the fields so produced are usually not transform limited, making it difficult to achieve temporal mode matching and thus resulting in reduced visibility of the interference. Optical filtering can force the pulses to be transform limited and thus improve the visibility. But the bandwidth of the optical filters must be narrow as compared to the pump bandwidth and down-conversion bandwidth [13]. Therefore, visibility of the interference depends on various parameters such as the filter bandwidth, pump field bandwidth, and the dispersion of the down-conversion medium. Perhaps because of such complicated dependence, a visibility of only about 70% has been observed so far in the interference between independent parametric down-conversion [5,7]. Since higher-order coincidence signal is usually quite low and whole interference pattern has to be recorded before the visibility can be extracted, the procedure to improve the visibility is proved to be extremely tedious and time consuming. In this paper, we will show that the visibility in a number of higher-order interference schemes is connected to a quantity that is a measure of photon bunching effect in one of the two down-converted fields. This quantity is easily measurable and will aid us in improving the visibility for higher-order interference between independent fields.

Photon bunching is a well-known higher-order effect usually associated with optical fields with thermal fluctuations [14]. It was proved that optical amplifier without input signal exhibits thermal fluctuation—spontaneous emission basically is of thermal nature [15]. It is also known that in parametric down-conversion processes, as far as only one beam is concerned, it behaves as an amplifier. Therefore, spontaneous parametric down-conversion should also exhibit photon bunching effect [16]. Such an effect has been ignored so far

in all the higher order measurement in parametric down-conversion because of the extremely wide bandwidth of down-converted fields (in the terahertz range). Superficially, there seems to be no connection between the photon bunching effect and the visibility of interference with the fields from parametric down-conversion. However, if we notice the conditions for the observation of photon bunching and for high visibility in interference between independent fields, they are startlingly similar: both require the bandwidth of the fields be much smaller than that of the detectors in the case of stationary fields. For nonstationary fields, the photon bunching effect has never been treated, especially for the pulsed parametric down-conversion process.

Most of the higher-order interference schemes investigated so far (including GHZ multi-particle interferometer) involve quantum interference between two paths (two waves). More interesting phenomena occur when more paths (waves) participate in interference, as in the diffraction pattern from a multiple slit ensemble (also known as optical grating) in contrast to Young's double slit interference pattern, and in the output of a Fabry-Perot interferometer compared to the output from a Michelson interferometer. As a matter of fact, in Shor's algorithm of quantum computing [8], multiple path interference effect similar to that in optical grating is used to ensure correct outcome with 100% certainty even though quantum process is usually associated with randomness. There have been some discussions on multi-path interference in a generalization of two-photon interference in a tritter where three paths are involved in interference [17].

In the following, we will first discuss the photon bunching effect in parametric down-conversion pumped by a pulse and find the condition for its observation. Then in Sec. III, we will consider a number of interference schemes involving interference between sources from two independent parametric down-conversion processes. The first one concerns two-photon interference between two independent signal fields of two parametric down-conversion process. The second one deals with the same situation but with coincidence detection gated on the simultaneous detection of two idler fields. The third and fourth schemes involve polarization interferometry related to quantum state teleportation [4,5] and entanglement swapping [6,7]. We will explore the connection between photon bunching effect and the visibilities of these interference schemes. In Sec. IV, we will investigate an interference scheme that involves four photons. We find that the size of the four-photon interference effect also relies on the photon bunching effect. In all of the above studies, we will utilize the theory recently developed for the parametric down-conversion process pumped by a coherent pulse [13].

II. PHOTON BUNCHING EFFECT IN PARAMETRIC DOWN-CONVERSION

The process of parametric down-conversion pumped by a coherent pulse can be described by the following state:

$$|\Psi\rangle = (1 - |\eta|^2/2)|\text{vac}\rangle + \eta|\Phi_1\rangle + \eta^2|\Phi_2\rangle \quad (2.1)$$

up to the first order of η (see later for the physical meaning of η) [13]. Here the states $|\Phi_{1,2}\rangle$ have the following form:

$$|\Phi_1\rangle = \int d\omega_1 d\omega_2 \Phi(\omega_1, \omega_2) \hat{a}_s^\dagger(\omega_1) \hat{a}_i^\dagger(\omega_2) |\text{vac}\rangle, \quad (2.2a)$$

$$|\Phi_2\rangle = \frac{1}{2} \int d\omega_1 d\omega_2 d\omega'_1 d\omega'_2 \Phi(\omega_1, \omega_2) \Phi(\omega'_1, \omega'_2) \times \hat{a}_s^\dagger(\omega_1) \hat{a}_i^\dagger(\omega_2) \hat{a}_s^\dagger(\omega'_1) \hat{a}_i^\dagger(\omega'_2) |\text{vac}\rangle. \quad (2.2b)$$

The information about the pump field and the parametric interaction is contained in the function $\Phi(\omega_1, \omega_2)$, which has the explicit form of

$$\Phi(\omega_1, \omega_2) = a_p(\omega_1 + \omega_2) \phi(\omega_1 + \omega_2, \omega_1 - \omega_2), \quad (2.3)$$

where $a_p(\omega)$ describes the pump field spectrum and $\phi(\omega_p, \omega)$ is the two-photon wave amplitude for single-frequency (ω_p) pumped parametric down-conversion. For near degenerate case, we have $\phi(\omega_p, \omega) = \phi(\omega_p, -\omega)$ so that $\Phi(\omega_1, \omega_2)$ has the exchange symmetry: $\Phi(\omega_1, \omega_2) = \Phi(\omega_2, \omega_1)$. The coherence property of the pump field is determined by the function $a_p(\omega)$. For stationary fields, $a_p(\omega)$ is a stochastic function of ω and satisfies the relation $\langle a(\omega) a^*(\omega') \rangle = I_p(\omega) \delta(\omega - \omega')$ with $I_p(\omega)$ the spectrum of the pump field. For a coherent pulse (transform limited), $a_p(\omega)$ is a well-behaved deterministic function of ω . Here the pump field is treated as a classical field. So for parametric down-conversion pumped by a coherent pulse, the function $\Phi(\omega_1, \omega_2)$ is a nonrandom function. Without loss of generality, we impose the normalization condition on $\Phi(\omega_1, \omega_2)$:

$$\int d\omega_1 d\omega_2 |\Phi(\omega_1, \omega_2)|^2 = 1, \quad (2.4)$$

so that both $|\Phi_1\rangle$ and $|\Phi_2\rangle$ are normalized.

To find out the physical meaning of η , let us first calculate the single photon detection rate of a single field of down-conversion. The electric field operators for the down-converted fields are given by

$$\hat{E}_s(t) = \frac{1}{\sqrt{2\pi}} \int d\omega \hat{a}_s(\omega) e^{-i\omega t}, \quad (2.5a)$$

$$\hat{E}_i(t) = \frac{1}{\sqrt{2\pi}} \int d\omega \hat{a}_i(\omega) e^{-i\omega t}. \quad (2.5b)$$

Then the probability rate of detecting a photon in the signal or idler field is given by

$$p_{1,s}(t) = \langle \Psi | \hat{E}_s^\dagger(t) \hat{E}_s(t) | \Psi \rangle = \|\hat{E}_s(t) | \Psi \rangle\|^2. \quad (2.6)$$

It can be easily calculated by using the state in Eq. (2.1) that to the first nonzero order of η , $p_{1,s}(t)$ has the form of

$$p_{1,s}(t) = \frac{|\eta|^2}{2\pi} \int d\omega_2 \left| \int d\omega_1 \Phi(\omega_1, \omega_2) e^{-i\omega_1 t} \right|^2. \quad (2.7)$$

Since the pump field is nonstationary (pulsed), the probability rate depends on time t . The overall probability of detecting a photon is the contribution from all time:

$$P_{1s} = \int_{-\infty}^{\infty} dt p_1(t) = |\eta|^2 \int d\omega_1 d\omega_2 |\Phi(\omega_1, \omega_2)|^2 = |\eta|^2, \quad (2.8)$$

where we used the normalization condition in Eq. (2.4) in evaluating the integral. Therefore, $|\eta|^2$ is simply the probability of photon conversion in a single pump pulse.

To see photon bunching in the signal or idler field, let us calculate the two-photon detection probability rate

$$p_{2s}(t_1, t_2) = \|\hat{E}_s(t_1)\hat{E}_s(t_2)|\Psi\rangle\|^2 = |\eta|^2 \|\hat{E}_s(t_1)\hat{E}_s(t_2)|\Phi_2\rangle\|^2, \quad (2.9)$$

where we used Eq. (2.1) for the state $|\Psi\rangle$. The states $|\text{vac}\rangle$ and $|\Phi_1\rangle$ do not contribute in Eq. (2.9). By making use of the commutation relation

$$[\hat{a}_s(\omega)\hat{a}_s(\omega'), \hat{a}_s^\dagger(\omega_1)\hat{a}_s^\dagger(\omega_1')] = \delta(\omega - \omega_1)\delta(\omega' - \omega_1') + \delta(\omega - \omega_1')\delta(\omega' - \omega_1), \quad (2.10)$$

we find the quantity in Eq. (2.9) as

$$p_{2s}(t_1, t_2) = \frac{|\eta|^4}{4(2\pi)^2} \int d\omega_2 d\omega_2' \{|F(\omega_2, \omega_2')|^2 + F(\omega_2, \omega_2')F^*(\omega_2', \omega_2)\}, \quad (2.11)$$

where

$$F(\omega_2, \omega_2') \equiv \int d\omega_1 d\omega_1' \Phi(\omega_1, \omega_2)\Phi(\omega_1', \omega_2') \times (e^{-i\omega_1 t_1 - \omega_1' t_2} + e^{-i\omega_1' t_1 - i\omega_1 t_2}). \quad (2.12)$$

Next, we calculate the overall probability for detecting two photons in one pump pulse by integrating the time variables t_1, t_2 over the pulse period and we obtain

$$P_{2s} = \int_{-\infty}^{\infty} dt_1 dt_2 p_{2s}(t_1, t_2) = \frac{|\eta|^4}{2(2\pi)^2} \int d\omega_2 d\omega_2' \int_{-\infty}^{\infty} dt_1 dt_2 |F(\omega_2, \omega_2')|^2. \quad (2.13)$$

Under the time integral, the contributions from the two terms in Eq. (2.11) are equal because of the symmetry among $t_1, t_2, \omega_1, \omega_1', \omega_2, \omega_2'$ in Eq. (2.12). After some lengthy calculation, Eq. (2.13) becomes

$$P_{2s} = |\eta|^4 \int d\omega_1 d\omega_1' d\omega_2 d\omega_2' [|\Phi(\omega_1, \omega_2)\Phi(\omega_1', \omega_2')|^2 + \Phi(\omega_1, \omega_2)\Phi(\omega_1', \omega_2')\Phi^*(\omega_1, \omega_2')\Phi^*(\omega_1', \omega_2)] \equiv \mathcal{A} + \mathcal{E}, \quad (2.14)$$

where

$$\mathcal{A} \equiv |\eta|^4 \int d\omega_1 d\omega_1' d\omega_2 d\omega_2' |\Phi(\omega_1, \omega_2)\Phi(\omega_1', \omega_2')|^2 = |\eta|^4 = P_{1s}^2 \quad (2.15)$$

is the accidental two-photon probability and

$$\mathcal{E} \equiv |\eta|^4 \int d\omega_1 d\omega_1' d\omega_2 d\omega_2' \Phi(\omega_1, \omega_2)\Phi(\omega_1', \omega_2') \times \Phi^*(\omega_1, \omega_2')\Phi^*(\omega_1', \omega_2) \quad (2.16)$$

is the excess two-photon probability due to photon bunching. Here normalization relation in Eq. (2.4) is used in Eq. (2.15). Notice that $\mathcal{E} \leq \mathcal{A}$ because of the Schwartz inequality. The equality holds if and only if the function $\Phi(\omega_1, \omega_2)$ can be factorized into $k(\omega_1)h(\omega_2)$. But this is impossible because of the complicated dependence of Φ on ω_1, ω_2 . However, with the help of narrow band filters before detection, we can modify the function of $\Phi(\omega_1, \omega_2)$. To see how, we need to carry out the above calculation with modified electric field operators as

$$\hat{E}_s(t) = \frac{1}{\sqrt{2\pi}} \int d\omega f(\omega - \omega_0) \hat{a}_s(\omega) e^{i\omega t}, \quad (2.17a)$$

$$\hat{E}_i(t) = \frac{1}{\sqrt{2\pi}} \int d\omega f(\omega - \omega_0) \hat{a}_i(\omega) e^{i\omega t}, \quad (2.17b)$$

instead of Eq. (2.5). Here $f(\omega - \omega_0)$ is the transmission function of the optical filters centered at the central down-conversion frequency ω_0 . It can be shown that if we do not apply the normalization condition of Eq. (2.4) to Eqs. (2.8) and (2.15), the formulas in Eqs. (2.8) and (2.14)–(2.16) for P_{1s} and P_{2s} are still correct so long as we change $\Phi(\omega_1, \omega_2)$ in Eq. (2.3) to

$$\Phi(\omega_1, \omega_2) = f(\omega_1)f(\omega_2)a_p(\omega_1 + \omega_2)\phi(\omega_1 + \omega_2, \omega_1 - \omega_2). \quad (2.18)$$

Therefore, we can make the ratio \mathcal{E}/\mathcal{A} approaching to 1 if we make the optical filter band width much narrower than those of $a_p(\omega)$ and $\phi(\omega, \omega')$ so that the dependence of $\Phi(\omega_1, \omega_2)$ on ω_1, ω_2 comes mainly from $f(\omega_1)f(\omega_2)$ and $\Phi(\omega_1, \omega_2)$ is factorized. Under this condition we have the perfect photon bunching:

$$g_2 \equiv P_{2s}/P_{1s}^2 = (\mathcal{A} + \mathcal{E})/\mathcal{A} = 2. \quad (2.19)$$

III. INTERFERENCE BETWEEN INDEPENDENT PARAMETRIC DOWN-CONVERSION SOURCES

Quantum interference between the correlated signal and idler fields from parametric down-conversion has been thoroughly studied. It has been demonstrated that high visibility can be easily achieved with careful balance of the propagation paths for the two fields. For interference between two independent parametric sources, we will show in the following that the visibility is associated with the quantity \mathcal{E}/\mathcal{A} discussed in the preceding section.

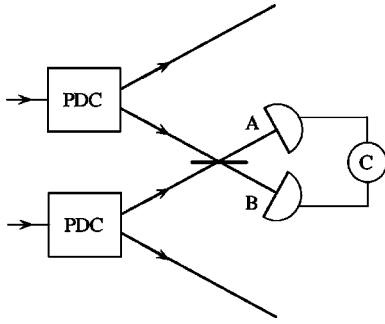


FIG. 1. Interference between two signal fields of two independent parametric processes.

A. Two-photon interference without gating

Consider two parametric processes pumped by a common pulse described by $a_p(\omega)$. The quantum state that describes the overall system is given by

$$|\Psi\rangle = |\Psi^{(1)}\rangle \otimes |\Psi^{(2)}\rangle, \quad (3.1)$$

where $|\Psi^{(1,2)}\rangle$ describes the quantum state from each parametric process and has the form of Eq. (2.1) with \hat{a}_s changed to \hat{a}_{s1} or \hat{a}_{s2} and \hat{a}_i changed to \hat{a}_{i1} or \hat{a}_{i2} .

We next superpose $s1$ and $s2$ fields with a beamsplitter but leave $i1$ and $i2$ fields unattended and observe two-photon coincidence between the two outputs of the beamsplitter (Fig. 1). The output fields of the beamsplitter are connected to $s1$ and $s2$ fields by

$$\hat{E}_A(t) = \frac{1}{\sqrt{2}}[\hat{E}_{s1}(t) + \hat{E}_{s2}(t + \tau)], \quad (3.2a)$$

$$\hat{E}_B(t) = \frac{1}{\sqrt{2}}[\hat{E}_{s2}(t) - \hat{E}_{s1}(t - \tau)], \quad (3.2b)$$

where we introduced a time delay τ so that the transmitted and the reflected fields arrive at the detectors at different times. This time delay is important because when τ is zero, we should have complete overlap of the two fields and maximum interference effect; but when τ is larger than the coherence time of the two fields, no interference should occur and it provides a base line for interference. So by comparing the coincidence at these two values of τ , we can deduce the visibility of the interference.

Two-photon coincidence between \hat{E}_A and \hat{E}_B fields is proportional to

$$p_2(t_1, t_2) = \|\hat{E}_A(t_1)\hat{E}_B(t_2)|\Psi\rangle\|^2. \quad (3.3)$$

Using Eq. (3.2), we have

$$\begin{aligned} & \hat{E}_A(t_1)\hat{E}_B(t_2) \\ &= \frac{1}{2}[\hat{E}_{s1}(t_1)\hat{E}_{s2}(t_2) - \hat{E}_{s2}(t_1 + \tau)\hat{E}_{s1}(t_2 - \tau) \\ & \quad + \hat{E}_{s2}(t_1 + \tau)\hat{E}_{s2}(t_2) - \hat{E}_{s1}(t_1)\hat{E}_{s1}(t_2 - \tau)]. \end{aligned} \quad (3.4)$$

Because of the existence of idler fields in $|\Psi\rangle$, it can be easily shown that in Eq. (3.3), the states $\hat{E}_{s1}\hat{E}_{s1}|\Psi\rangle$, $\hat{E}_{s2}\hat{E}_{s2}|\Psi\rangle$, and $(\hat{E}_{s1}\hat{E}_{s2} - \hat{E}_{s2}\hat{E}_{s1})|\Psi\rangle$ are mutually orthogonal. So we have

$$\begin{aligned} p_2(t_1, t_2) &= \frac{1}{4}\{ \|\hat{E}_{s1}(t_1)\hat{E}_{s1}(t_2 - \tau)|\Psi\rangle\|^2 \\ & \quad + \|\hat{E}_{s2}(t_1 + \tau)\hat{E}_{s2}(t_2)|\Psi\rangle\|^2 \\ & \quad + \|\hat{E}_{s1}(t_1)\hat{E}_{s2}(t_2) - \hat{E}_{s2}(t_1 + \tau) \\ & \quad \times \hat{E}_{s1}(t_2 - \tau)|\Psi\rangle\|^2 \}. \end{aligned} \quad (3.5)$$

If the coincidence window is much larger than the coherence time of the down-converted fields, which is usually the case in experiment, the observed coincidence is a time average of $p_2(t_1, t_2)$:

$$P_2(\tau) = \int_{-\infty}^{\infty} dt_1 dt_2 p_2(t_1, t_2). \quad (3.6)$$

Under the time average, the contributions from the first two terms in Eq. (3.5) have been calculated in Eqs. (2.9) and (2.14). We simply rewrite the result as follows:

$$\begin{aligned} & \int dt_1 dt_2 \|\hat{E}_{s1}(t_1)\hat{E}_{s1}(t_2 - \tau)|\Psi\rangle\|^2 \\ &= \int dt_1 dt_2 \|\hat{E}_{s2}(t_1 + \tau)\hat{E}_{s2}(t_2)|\Psi\rangle\|^2 \\ &= \mathcal{A} + \mathcal{E}. \end{aligned} \quad (3.7)$$

Notice that these two terms are independent of the time delay τ and provide the base line for interference fringe. The contribution from the last term in Eq. (3.5) gives rise to interference. To calculate it, we start with $\hat{E}_{s1}(t_1)\hat{E}_{s2}(t_2)|\Psi\rangle$:

$$\begin{aligned} & \hat{E}_{s1}(t_1)\hat{E}_{s2}(t_2)|\Psi\rangle \\ &= \hat{E}_{s1}(t_1)|\Psi^{(1)}\rangle\hat{E}_{s2}(t_2)|\Psi^{(2)}\rangle \\ &= \frac{\eta^2}{2\pi} \int d\omega_1 d\omega_2 \Phi(\omega_1, \omega_2) e^{-i\omega_1 t_1} \hat{a}_{i1}^\dagger(\omega_2) |\text{vac}^{(1)}\rangle \\ & \quad \times \int d\omega'_1 d\omega'_2 \Phi(\omega'_1, \omega'_2) e^{-i\omega'_1 t_2} \hat{a}_{i2}^\dagger(\omega'_2) |\text{vac}^{(2)}\rangle \\ &= \frac{\eta^2}{2\pi} \int d\omega_1 d\omega_2 d\omega'_1 d\omega'_2 \Phi(\omega_1, \omega_2) \Phi(\omega'_1, \omega'_2) \\ & \quad \times e^{-i\omega_1 t_1 - i\omega'_1 t_2} \hat{a}_{i1}^\dagger(\omega_2) \hat{a}_{i2}^\dagger(\omega'_2) |\text{vac}\rangle. \end{aligned} \quad (3.8)$$

For the other term, we can obtain it by simply replacing t_1 with $t_2 - \tau$ and t_2 with $t_1 + \tau$ in Eq. (3.8). So we have

$$\begin{aligned} & \|[\hat{E}_{s1}(t_1)\hat{E}_{s2}(t_2) - \hat{E}_{s2}(t_1 + \tau)\hat{E}_{s1}(t_2 - \tau)]|\Psi\rangle\|^2 \\ &= \frac{|\eta|^4}{(2\pi)^2} \int d\omega_2 d\omega'_2 \left| \int d\omega_1 d\omega'_1 \Phi(\omega_1, \omega_2) \Phi(\omega'_1, \omega'_2) \right. \\ & \quad \left. \times [e^{-i\omega_1 t_1 - i\omega'_1 t_2} - e^{-i\omega_1(t_2 - \tau) - i\omega'_1(t_1 + \tau)}] \right|^2 \end{aligned}$$

$$\begin{aligned}
&= \frac{|\eta|^4}{(2\pi)^2} \int d\omega_2 d\omega'_2 \left| \int d\omega_1 d\omega'_1 e^{-i\omega_1 t_1 - i\omega'_1 t_2} \right. \\
&\quad \times [\Phi(\omega_1, \omega_2) \Phi(\omega'_1, \omega'_2) \\
&\quad \left. - \Phi(\omega'_1, \omega_2) \Phi(\omega_1, \omega'_2) e^{i(\omega'_1 - \omega_1)\tau}] \right|^2, \quad (3.9)
\end{aligned}$$

where we used the fact that $\{\hat{a}_{i1}^\dagger(\omega_2) \hat{a}_{i2}^\dagger(\omega'_2) | \text{vac}\rangle\}$ is a set of orthogonal states and we made the switch $\omega_1 \leftrightarrow \omega'_1$ in the second term in the integrand. Now we can carry out the time average. The result is

$$\begin{aligned}
&\int dt_1 dt_2 ||[\hat{E}_{s1}(t_1) \hat{E}_{s2}(t_2) - \hat{E}_{s2}(t_1 + \tau) \hat{E}_{s1}(t_2 - \tau)] |\Psi\rangle ||^2 \\
&= |\eta|^4 \int d\omega_1 d\omega'_1 d\omega_2 d\omega'_2 [\Phi(\omega_1, \omega_2) \Phi(\omega'_1, \omega'_2) \\
&\quad - \Phi(\omega'_1, \omega_2) \Phi(\omega_1, \omega'_2) e^{i(\omega'_1 - \omega_1)\tau}]^2 \\
&= 2[\mathcal{A} - \mathcal{E}(\tau)] \quad (3.10)
\end{aligned}$$

with

$$\begin{aligned}
\mathcal{E}(\tau) &\equiv |\eta|^4 \text{Re} \int d\omega_1 d\omega'_1 d\omega_2 d\omega'_2 \Phi(\omega_1, \omega_2) \\
&\quad \times \Phi(\omega'_1, \omega'_2) \Phi^*(\omega'_1, \omega_2) \\
&\quad \times \Phi^*(\omega_1, \omega'_2) e^{i(\omega_1 - \omega'_1)\tau}. \quad (3.11)
\end{aligned}$$

Notice that $\mathcal{E}(0) = \mathcal{E}$, and $\mathcal{E}(\infty) = 0$ if $\Phi(\omega_1, \omega_2)$ has a finite bandwidth. Combining Eqs. (3.5)–(3.7) and (3.10), we find the overall coincidence proportional to

$$P_2(\tau) = \mathcal{A} + \frac{1}{2}[\mathcal{E} - \mathcal{E}(\tau)]. \quad (3.12)$$

Therefore, as the time delay τ scans through 0 from $-\infty$ to $+\infty$, the coincidence will show a dip at $\tau=0$ with a minimum value of \mathcal{A} . The baseline for the coincidence is at $\tau = \pm\infty$ with a value of $\mathcal{A} + \mathcal{E}/2$. So the visibility of the interference pattern is

$$v = \frac{P_2(\infty) - P_2(0)}{P_2(\infty)} = \frac{\mathcal{E}}{2\mathcal{A} + \mathcal{E}}. \quad (3.13)$$

Since $\mathcal{E} \leq \mathcal{A}$, the maximum value of v is 1/3. This value is consistent with the theory of fourth-order interference between two thermal fields.

B. Two-photon interference with gating

In the interference scheme discussed in the preceding part, the two signal fields from two independent parametric down-conversion are used without any participation of the conjugate idler fields. So the two fields are of thermal nature. However, if we can gate the coincidence measurement on the detection of the two idler fields in the two parametric process, the gated signal fields will be in a single-photon Fock state [18] and the situation has no difference from the correlated two-photon case [19]. We should expect the visibility

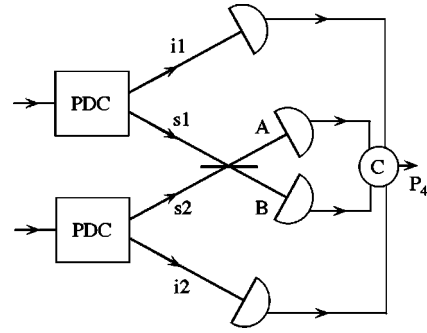


FIG. 2. Interference between two signal fields of two independent parametric processes gated upon the detection of two idler fields.

of the interference reach 100% in ideal condition and the coincidence will dip down to zero at zero delay ($\tau=0$). This interference scheme together with the one in part A has been recently implemented experimentally by Rhee and Wang [20]. In the following, we will calculate the visibility in this interference scheme and relate it to the quantities \mathcal{A} and \mathcal{E} .

If we gate the coincidence measurement on the detection of the two idler photons, this corresponds to quadruple coincidence measurement of two output fields of the beamsplitter and two idler fields (Fig. 2). The coincidence rate is proportional to

$$p_4(t_1, t_2, t_3, t_4) = ||\hat{E}_A(t_1) \hat{E}_B(t_2) \hat{E}_{i1}(t_3) \hat{E}_{i2}(t_4) |\Psi\rangle ||^2. \quad (3.14)$$

To calculate p_4 , we can make use of Eq. (3.4) for $\hat{E}_A(t_1) \hat{E}_B(t_2)$. But it can be easily shown that there is no contribution from the last two terms, that is,

$$\hat{E}_{s1}(t_1) \hat{E}_{s1}(t_2 - \tau) \hat{E}_{i1}(t_3) \hat{E}_{i2}(t_4) |\Psi\rangle = 0 \quad (3.15)$$

and

$$\hat{E}_{s2}(t_1 + \tau) \hat{E}_{s2}(t_2) \hat{E}_{i1}(t_3) \hat{E}_{i2}(t_4) |\Psi\rangle = 0 \quad (3.16)$$

up to the order of η^2 because of the two-photon nature of $|\Phi_1^{(1,2)}\rangle$ in Eq. (2.2a). For the contribution from the first two terms, we have

$$\begin{aligned}
&[\hat{E}_{s1}(t_1) \hat{E}_{s2}(t_2) - \hat{E}_{s2}(t_1 + \tau) \hat{E}_{s1}(t_2 - \tau)] \hat{E}_{i1}(t_3) \hat{E}_{i2}(t_4) |\Psi\rangle \\
&= \frac{\eta^2}{(2\pi)^2} \int d\omega_1 d\omega'_1 d\omega_2 d\omega'_2 \Phi(\omega_1, \omega_2) \Phi(\omega'_1, \omega'_2) \\
&\quad \times [e^{-i\omega_1 t_1 - i\omega'_1 t_2 - i\omega_2 t_3 - i\omega'_2 t_4} \\
&\quad - e^{-i\omega'_1(t_1 + \tau) - i\omega_1(t_2 - \tau) - i\omega_2 t_3 - i\omega'_2 t_4}] | \text{vac}\rangle \\
&= \frac{\eta^2}{(2\pi)^2} \int d\omega_1 d\omega'_1 d\omega_2 d\omega'_2 [\Phi(\omega_1, \omega_2) \Phi(\omega'_1, \omega'_2) \\
&\quad - \Phi(\omega'_1, \omega_2) \Phi(\omega_1, \omega'_2) e^{i(\omega'_1 - \omega_1)\tau}] \\
&\quad \times e^{-i\omega_1 t_1 - i\omega'_1 t_2 - i\omega_2 t_3 - i\omega'_2 t_4} | \text{vac}\rangle. \quad (3.17)
\end{aligned}$$

So the probability rate is

$$p_4(t_1, t_2, t_3, t_4) = \frac{|\eta|^4}{4(2\pi)^4} \left| \int d\omega_1 d\omega'_1 d\omega_2 d\omega'_2 [\Phi(\omega_1, \omega_2) \Phi(\omega'_1, \omega'_2) - \Phi(\omega'_1, \omega_2) \Phi(\omega_1, \omega'_2) e^{i(\omega'_1 - \omega_1)\tau}] e^{-i\omega_1 t_1 - i\omega'_1 t_2 - i\omega_2 t_3 - i\omega'_2 t_4} \right|^2 \quad (3.18)$$

and the overall quadruple detection probability in one pulse is the time average over the pulse duration and is calculated to be

$$P_4(\tau) = \frac{|\eta|^4}{4} \int d\omega_1 d\omega'_1 d\omega_2 d\omega'_2 |\Phi(\omega_1, \omega_2) \Phi(\omega'_1, \omega'_2) - \Phi(\omega'_1, \omega_2) \Phi(\omega_1, \omega'_2) e^{i(\omega'_1 - \omega_1)\tau}|^2 = \frac{1}{2} [\mathcal{A} - \mathcal{E}(\tau)], \quad (3.19)$$

where \mathcal{A} and $\mathcal{E}(\tau)$ are the quantities defined in Eq. (2.15) and Eq. (3.11), respectively. As expected, the gated detection takes out the extra τ -independent contribution given in Eq. (3.7) to the overall coincidence. Therefore, the visibility of the interference fringe is

$$v = \mathcal{E}/\mathcal{A}. \quad (3.20)$$

In the ideal case when $\mathcal{E} = \mathcal{A}$, we will have $v = 1$, i.e., 100% visibility, which is exactly what we expect for the interference of two Fock states. Notice that the visibility is directly connected to the photon bunching quantity \mathcal{E}/\mathcal{A} . Such a connection has been demonstrated recently by Rhee and Wang [20].

C. Quantum state teleportation and entanglement swapping

Another type of interference effect between independent fields from parametric down-conversion involves polarization entanglement. Interference occurs by projecting fields with correlated polarization into certain common direction. Quantum superposition stems from projection of fields of different polarizations. Violation of Bell's inequality by Bohm-type EPR state is related to two-photon interference of correlated sources with different polarizations. Quantum state teleportation and entanglement swapping [4–7] are very similar but involve independent sources. The underlying principle is the same as discussed in the previous part. Although multimode calculation was performed before on these [21], we want to present them here again to derive the visibility of the interference in terms of the quantities \mathcal{A} and \mathcal{E} that are associated with photon bunching effect.

Quantum teleportation of an arbitrary single photon polarization state $|\theta_1\rangle = \cos \theta_1 |x\rangle + \sin \theta_1 |y\rangle$ was first proposed by Bennett *et al.* and recently demonstrated by Bouwmeester *et al.* [5]. The schematics is shown in Fig. 3. Two parametric down-converters are used in the demonstration. The first one prepares a single photon polarization state $|\theta_1\rangle_{s1} = \cos \theta_1 |x\rangle_{s1} + \sin \theta_1 |y\rangle_{s1}$ in $s1$ by gating all the measurement on the detection of $i1$. The second one produces a Bohm-EPR singlet state: $|EPR\rangle = (|x_{s2}, y_{i2}\rangle - |y_{s2}, x_{i2}\rangle)/\sqrt{2}$. By

gating on the outcome of the Bell measurement of $s1$ and $s2$, the state of $i2$ is expected to be projected into $|\theta_1\rangle_{i2} = \cos \theta_1 |x\rangle_{i2} + \sin \theta_1 |y\rangle_{i2}$, thus achieving teleportation. The output polarization state in $i2$ can be checked by making a polarization measurement in direction θ_2 . By Malus law, we should have the detection rate after the polarizer proportional to $\cos^2(\theta_1 - \theta_2)$. Bell measurement on $s1$ and $s2$ is achieved by superposing the two fields with a beamsplitter and measuring the coincidence between the two outputs of the beamsplitter [21]. Notice the similarity in the arrangement between Figs. 2 and 3. The difference only lies in the polarization measurement on $i2$ and the state of down-conversion.

The multimode description of the down-conversion states is similar to Eq. (2.1). To cope with the polarization state of the fields, we introduce extra degree of freedom for polarization entanglement. The quantum state of the system is given by

$$|\Psi\rangle = |\Psi^{(1)}\rangle \otimes |\Psi^{(2)}\rangle, \quad (3.21)$$

with

$$|\Psi^{(1)}\rangle = \eta \int d\omega_1 d\omega_2 \Phi(\omega_1, \omega_2) [\hat{a}_{s1x}^\dagger(\omega_1) \cos \theta_1 + \hat{a}_{s1y}^\dagger(\omega_1) \sin \theta_1] \hat{a}_{i1}^\dagger(\omega_2) |\text{vac}\rangle. \quad (3.22)$$

$$|\Psi^{(2)}\rangle = \frac{\eta}{\sqrt{2}} \int d\omega'_1 d\omega'_2 \Phi(\omega'_1, \omega'_2) [\hat{a}_{s2x}^\dagger(\omega'_1) \hat{a}_{i2y}^\dagger(\omega'_2) - \hat{a}_{s2y}^\dagger(\omega'_1) \hat{a}_{i2x}^\dagger(\omega'_2)] |\text{vac}\rangle. \quad (3.23)$$

Here we only consider the second term in Eq. (2.1) for the two parametric down-conversion processes. The function $\Phi(\omega_1, \omega_2)$ is same as in Eq. (2.3). So the state of the system becomes

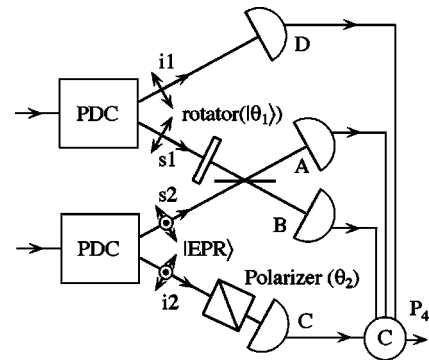


FIG. 3. Scheme of quantum state teleportation with two independent parametric down-conversion processes.

$$\begin{aligned}
|\Psi\rangle = & \frac{\eta^2}{\sqrt{2}} \int d\omega_1 d\omega_2 d\omega'_1 d\omega'_2 \Phi(\omega_1, \omega_2) \Phi(\omega'_1, \omega'_2) \\
& \times [\hat{a}_{s1x}^\dagger(\omega_1) \hat{a}_{i1}^\dagger(\omega_2) \hat{a}_{s2x}^\dagger(\omega'_1) \hat{a}_{i2y}^\dagger(\omega'_2) \cos \theta_1 \\
& + \hat{a}_{s1y}^\dagger(\omega_1) \hat{a}_{i1}^\dagger(\omega_2) \hat{a}_{s2x}^\dagger(\omega'_1) \hat{a}_{i2y}^\dagger(\omega'_2) \sin \theta_1 \\
& - \hat{a}_{s1x}^\dagger(\omega_1) \hat{a}_{i1}^\dagger(\omega_2) \hat{a}_{s2y}^\dagger(\omega'_1) \hat{a}_{i2x}^\dagger(\omega'_2) \cos \theta_1 \\
& - \hat{a}_{s1y}^\dagger(\omega_1) \hat{a}_{i1}^\dagger(\omega_2) \hat{a}_{s2y}^\dagger(\omega'_1) \hat{a}_{i2x}^\dagger(\omega'_2) \sin \theta_1] |\text{vac}\rangle.
\end{aligned} \tag{3.24}$$

Similar to Eq. (3.4), we have for the fields of two outputs of the beamsplitter

$$\hat{E}_{Ax}(t) = \frac{1}{\sqrt{2}} [\hat{E}_{s1x}(t) + \hat{E}_{s2x}(t + \tau)], \tag{3.25a}$$

$$\hat{E}_{Bx}(t) = \frac{1}{\sqrt{2}} [\hat{E}_{s2x}(t) - \hat{E}_{s1x}(t - \tau)], \tag{3.25b}$$

$$\hat{E}_{Ay}(t) = \frac{1}{\sqrt{2}} [\hat{E}_{s1y}(t) + \hat{E}_{s2y}(t + \tau)], \tag{3.25c}$$

$$\hat{E}_{By}(t) = \frac{1}{\sqrt{2}} [\hat{E}_{s2y}(t) - \hat{E}_{s1y}(t - \tau)], \tag{3.25d}$$

with

$$\hat{E}_j(t) = \frac{1}{\sqrt{2\pi}} \int d\omega \hat{a}_j(\omega) e^{-i\omega t} \quad (j = s1x, s1y, s2x, s2y). \tag{3.26}$$

Here because two polarizations are involved, we consider both of them in the field operators. The gated detection rate at detector C for the polarization measurement is proportional to the four-photon coincidence rate

$$p_4(t_1, t_2, t_3, t_4) = \langle \hat{I}_A(t_1) \hat{I}_B(t_2) \hat{I}_C(t_3) \hat{I}_D(t_4) \rangle, \tag{3.27}$$

where

$$\hat{I}_A = \hat{E}_{Ax}^\dagger \hat{E}_{Ax} + \hat{E}_{Ay}^\dagger \hat{E}_{Ay},$$

$$\hat{I}_B = \hat{E}_{Bx}^\dagger \hat{E}_{Bx} + \hat{E}_{By}^\dagger \hat{E}_{By},$$

$$\hat{I}_C = \hat{E}_C^\dagger \hat{E}_C,$$

$$\hat{I}_D = \hat{E}_{i1}^\dagger \hat{E}_{i1},$$

with

$$\hat{E}_C(t) = \frac{1}{\sqrt{2\pi}} \int d\omega [\hat{a}_{i2x}(\omega) \cos \theta_2 + \hat{a}_{i2y}(\omega) \sin \theta_2] e^{-i\omega t} \tag{3.28}$$

and

$$\hat{E}_{i1}(t) = \frac{1}{\sqrt{2\pi}} \int d\omega \hat{a}_{i1}(\omega) e^{-i\omega t}. \tag{3.29}$$

The expansion of the product $\hat{I}_A(t_1) \hat{I}_B(t_2)$ gives rise to four terms

$$\begin{aligned}
\hat{I}_A(t_1) \hat{I}_B(t_2) = & \hat{E}_{Ax}^\dagger \hat{E}_{Bx}^\dagger \hat{E}_{Ax} \hat{E}_{Bx} + \hat{E}_{Ay}^\dagger \hat{E}_{By}^\dagger \hat{E}_{Ay} \hat{E}_{By} \\
& + \hat{E}_{Ax}^\dagger \hat{E}_{By}^\dagger \hat{E}_{Ax} \hat{E}_{By} + \hat{E}_{Ay}^\dagger \hat{E}_{Bx}^\dagger \hat{E}_{Ay} \hat{E}_{Bx}.
\end{aligned} \tag{3.30}$$

Substituting Eq. (3.30) into Eq. (3.27), we have

$$\begin{aligned}
p_4(t_1, t_2, t_3, t_4) = & \|\hat{E}_{Ax}(t_1) \hat{E}_{Bx}(t_2) \hat{E}_C(t_3) \hat{E}_D(t_4) |\Psi\rangle\|^2 \\
& + \|\hat{E}_{Ay}(t_1) \hat{E}_{By}(t_2) \hat{E}_C(t_3) \hat{E}_D(t_4) |\Psi\rangle\|^2 \\
& + \|\hat{E}_{Ax}(t_1) \hat{E}_{By}(t_2) \hat{E}_C(t_3) \hat{E}_D(t_4) |\Psi\rangle\|^2 \\
& + \|\hat{E}_{Ay}(t_1) \hat{E}_{Bx}(t_2) \hat{E}_C(t_3) \hat{E}_D(t_4) |\Psi\rangle\|^2.
\end{aligned} \tag{3.31}$$

The overall probability is the time average over the pulse period and is given by

$$P_4(\tau, \theta_1, \theta_2) = \int_{-\infty}^{\infty} dt_1 dt_2 dt_3 dt_4 p_4(t_1, t_2, t_3, t_4). \tag{3.32}$$

Besides the subscripts $\{x, y\}$, each term in Eq. (3.31) is similar to Eq. (3.14). We can follow the same procedure to calculate their contributions to the overall probability. Due to complexity, we omit the detail of the calculation here and present the results as follows:

$$P_4(\text{1st term}) = \alpha [\mathcal{A} - \mathcal{E}(\tau)] \cos^2 \theta_1 \sin^2 \theta_2,$$

$$P_4(\text{2nd term}) = \alpha [\mathcal{A} - \mathcal{E}(\tau)] \sin^2 \theta_1 \cos^2 \theta_2,$$

$$P_4(\text{3rd term}) = P_4(\text{4th term})$$

$$\begin{aligned}
= & \frac{\alpha}{2} [\mathcal{A} (\cos^2 \theta_1 \cos^2 \theta_2 + \sin^2 \theta_1 \sin^2 \theta_2) \\
& + 2\mathcal{E}(\tau) \cos \theta_1 \cos \theta_2 \sin \theta_1 \sin \theta_2].
\end{aligned} \tag{3.33}$$

Here α is a proportional constant. So the overall probability becomes

$$P_4(\tau, \theta_1, \theta_2) = \alpha [\mathcal{A} - \mathcal{E}(\tau) \sin^2(\theta_1 - \theta_2)]. \tag{3.34}$$

In the ideal case when $\tau=0$ and $\mathcal{E}=\mathcal{A}$, we have

$$P_4(\theta_1, \theta_2) = \alpha \mathcal{A} \cos^2(\theta_1 - \theta_2), \tag{3.35}$$

which is exactly what we expect for the output of the polarizer in field $i2$ if the input state to the polarizer is $|\theta_1\rangle_{i2} = \cos \theta_1 |x\rangle_{i2} + \sin \theta_1 |y\rangle_{i2}$. Therefore, we achieved the teleportation of the state $|\theta_1\rangle$ from $i1$ to $i2$. In a recent experimen-

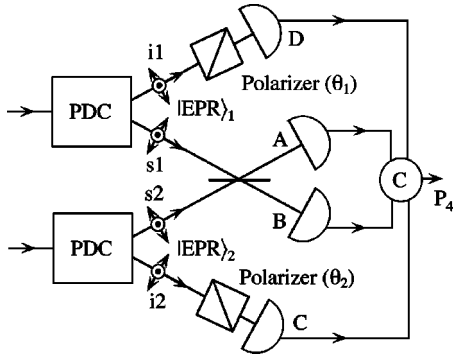


FIG. 4. Scheme of entanglement swapping with two independent parametric down-conversion processes.

tal demonstration of teleportation [5], θ_1 is fixed at $\pi/4$ and θ_2 is varied. From Eq. (3.34), we have with $\tau=0$ and $\theta_1 = \pi/4$

$$P_4(\theta_2) = \frac{\alpha}{2}(2\mathcal{A} - \mathcal{E} + \mathcal{E} \sin 2\theta_2). \quad (3.36)$$

When we scan θ_2 , P_4 exhibits sinusoidal oscillation with visibility

$$v = \frac{\mathcal{E}}{2\mathcal{A} - \mathcal{E}}. \quad (3.37)$$

Entanglement swapping [6,7] is similar to teleportation. The only difference is that in entanglement swapping, part of a correlated state is teleported while a whole polarization state is teleported in the simple scheme of quantum state teleportation. Specifically, the state to be teleported in entanglement swapping is an EPR correlated state (Fig. 4). By making Bell measurement on $s1$ and $s2$ and gating the polarization measurement of $i2$ on the result of the Bell measurement, we can transfer (swap) the EPR correlation between $i1$ and $s1$ to the EPR correlation between $i1$ and $i2$ even though $i1$ and $i2$ are independent of each other. This scheme can also be used for an ‘‘event-ready’’ Bell experiment, where the signal from the Bell measurement indicates that the EPR pair is ready for the test [6,22].

To confirm the EPR correlation between $i1$ and $i2$, we need perform polarization correlation measurement on both $i1$ and $i2$ and gate the measurement on the Bell measurement of $s1$ and $s2$ (quadruple coincidence measurement). The multimode description of the fields is similar to Eq. (3.21) except that $|\Psi^{(1)}\rangle$ is an EPR state similar to Eq. (3.23), that is,

$$|\Psi^{(1)}\rangle = \frac{\eta}{\sqrt{2}} \int d\omega_1 d\omega_2 \Phi(\omega_1, \omega_2) [\hat{a}_{s1x}^\dagger(\omega_1) \hat{a}_{i1y}^\dagger(\omega_2) - \hat{a}_{s1y}^\dagger(\omega_1) \hat{a}_{i1x}^\dagger(\omega_2)] |\text{vac}\rangle. \quad (3.38)$$

The fields for A, B, C are the same as in Eqs. (3.25) and (3.28), but the field D is changed to

$$\hat{E}_D(t) = \int d\omega [\hat{a}_{i1x}(\omega) \cos \theta_1 + \hat{a}_{i1y}(\omega) \sin \theta_1] e^{-i\omega t} \quad (3.39)$$

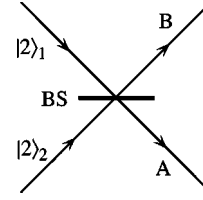


FIG. 5. Scheme of four-photon partition at a 50:50 beamsplitter.

for polarization measurement of $i1$. Following the same calculation leading to Eq. (3.34), we have for the quadruple measurement

$$P_4(\tau, \theta_1, \theta_2) = \alpha[\mathcal{A} - \mathcal{E}(\tau) \cos^2(\theta_1 - \theta_2)]. \quad (3.40)$$

In the ideal case when $\tau=0$ and $\mathcal{E}=\mathcal{A}$, we have

$$P_4(\theta_1, \theta_2) = \alpha \mathcal{A} \sin^2(\theta_1 - \theta_2), \quad (3.41)$$

which is exactly the polarization correlation for the EPR singlet state $|\text{EPR}\rangle = (|x_{i1}, y_{i2}\rangle - |y_{i1}, x_{i2}\rangle)/\sqrt{2}$. For less than ideal case, we set $\theta_1 = \pi/4$ and look at P_4 as a function of θ_2 , as in a recent experimental demonstration [7]. $P_4(\theta_2)$ will be a sinusoidal function of θ_2 :

$$P_4(\pi/4, \theta_2) = \frac{\alpha}{2}(2\mathcal{A} - \mathcal{E} - \mathcal{E} \sin 2\theta_2). \quad (3.42)$$

So the visibility of the modulation is then $v = \mathcal{E}/(2\mathcal{A} - \mathcal{E})$, which is same as in Eq. (3.37). As can be seen, the visibility in both quantum state teleportation and entanglement swapping is related to the quantity \mathcal{E}/\mathcal{A} , as in other interference schemes discussed in parts A and B.

IV. FOUR-PHOTON MULTIPATH INTERFERENCE

So far our discussion has been limited to two-photon interference. Even for the schemes in parts B and C, although quadruple coincidence is measured, it is still two-photon amplitudes that are involved in interference. Next we consider an interference scheme where four-photon amplitudes are superposed so that it corresponds to four-photon interference.

Consider now the situation when two pairs of photons enter a 50:50 beamsplitter (BS) with each pair in one input port (Fig. 5). We can treat the input state as photon number Fock state and in the simple single mode description, it has the form of $|2_1, 2_2\rangle$. Here 1,2 denote the two input modes of the BS. It can be easily shown [23] that the output state is given by

$$|\Phi\rangle = \sqrt{\frac{3}{8}}(|4_A, 0_B\rangle + |0_A, 4_B\rangle) + \frac{1}{2}|2_A, 2_B\rangle, \quad (4.1)$$

where the subscripts $\{A, B\}$ denote the two output modes. Notice that the states $|3_A, 1_B\rangle$ and $|1_A, 3_B\rangle$ are missing in Eq. (4.1). This can be easily understood in terms of two-photon interference. Recall that for an input state of $|1_1, 1_2\rangle$ to the BS, the output state is given by [19]

$$|\Phi\rangle = \frac{1}{\sqrt{2}}(|2_A, 0_B\rangle + |0_A, 2_B\rangle). \quad (4.2)$$

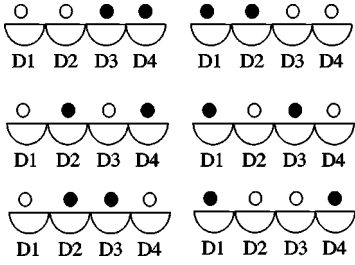


FIG. 6. Six possible ways to arrange two pairs of photons with four detectors for multipath four-photon interference.

If we consider the state $|2_1, 2_2\rangle$ as two pairs of photon with each pair in the state $|1_1, 1_2\rangle$, then according to Eq. (4.2), only $|4_A, 0_B\rangle$, $|0_A, 4_B\rangle$, and $|2_A, 2_B\rangle$ are possible. The disappearance of $|3_A, 1_B\rangle$ and $|1_A, 3_B\rangle$ terms in Eq. (4.1) is a direct result of the absence of $|1_A, 1_B\rangle$ term in Eq. (4.2) due to two-photon interference. This picture of two pairs of photons is usually referred to as 2×2 situation. However, such a picture is inappropriate in explaining the probability for $|4_A, 0_B\rangle$ and $|0_A, 4_B\rangle$. For, from Eq. (4.2) the probability for $|2_A, 0_B\rangle$ is $1/2$ for one pair, so the probability for $|4_A, 0_B\rangle$ is simply $(1/2)^2 = 1/4$ for two pairs. But from Eq. (4.1) the probability for $|4_A, 0_B\rangle$ is $3/8$. The difference comes from the fact that the four photons in the 2×2 case corresponds to two independent (uncorrelated) pairs while the four photons in $|2_1, 2_2\rangle$ are correlated.

To understand the partition probability for $|4_A, 0_B\rangle$ output state, we first treat the four photons as classical particles and consider the classical partition probability. As classical particles, the four photons can be thought of as independent particles and their partition at the BS simply follows Bernoulli distribution and $P_4 = (1/2)^2 = 1/16$. The ratio between quantum and classical predictions is then

$$P_4^q/P_4^c = 6. \quad (4.3)$$

We can understand the sixfold increase for quantum prediction in terms of four-photon interference: if we consider the two photons entering each side of the BS indistinguishable, then there are six possible ways to arrange the four photons (Fig. 6). The four numbered slots for the four photons can be viewed as four photodetectors. Since the four photons in the state $|4_A, 0_B\rangle$ are indistinguishable, the amplitudes for the six possibilities are added to give an overall amplitude of $6A$ due to constructive four-photon interference. Here A is the probability amplitude for each possibility. So the overall probability for $|4_A, 0_B\rangle$ is then $P_4^q = (6A)^2 = 36A^2$ for quantum prediction. However, for classical particles, there is no interference and we simply add probability A^2 for each possibility to obtain overall probability $P_4^c = 6A^2$. So we have the ratio $P_4^q/P_4^c = 36A^2/6A^2 = 6$, or sixfold increase from classical prediction to quantum prediction.

The four-photon interference picture discussed above can be also applied to the three other situations of $|3_A, 1_B\rangle$, $|1_A, 3_B\rangle$, and $|2_A, 2_B\rangle$ in Eq. (4.1). But because the three situations involve different combinations of reflected photons, which experience an extra $\pi/2$ phase shift for a symmetric beamsplitter, the probability amplitudes for the six possibilities in Fig. 6 will have different phases. For example, in the case of $|3_A, 1_B\rangle$, the total phases (experienced

by all four photons) for each probability amplitude of the six possibilities in Fig. 6 (D4 is now placed in side B) are $\pi/2, 3(\pi/2), \pi/2, 3(\pi/2), 3(\pi/2), \pi/2$, respectively. This results in probability amplitudes of $iA, -iA, iA, -iA, -iA, iA$ and a total probability amplitude of $iA - iA + iA - iA - iA + iA = 0$, which explains the disappearance of $|3_A, 1_B\rangle$ and $|1_A, 3_B\rangle$ terms in Eq. (4.1). We can likewise explain the coefficient for $|2_A, 2_B\rangle$ term.

To produce the state $|2_1, 2_2\rangle$, we can use parametric process in the higher order. The last term in Eq. (2.1), i.e., $|\Phi_2\rangle$ is a state of the form of $|2_s, 2_i\rangle$. However, the state is a multimode state. We need to treat the problem with a multimode theory. Because there is a more profound difference among P_4^q (four-photon interference), P_4^c (no interference), and $P_{2 \times 2}$ (the prediction from two-photon interference) for the $|4_A, 0_B\rangle$ or $|0_A, 4_B\rangle$ case, we will only study this case in the following multimode treatment.

Consider the quadruple detection probability at one output port (say, port A) of the beamsplitter:

$$p_4(t_1, t_2, t_3, t_4) = ||\hat{E}_A(t_1)\hat{E}_A(t_2)\hat{E}_A(t_3)\hat{E}_A(t_4)|\Psi\rangle||^2, \quad (4.4)$$

where

$$\hat{E}_A(t) = \frac{1}{\sqrt{2}}[\hat{E}_s(t) + \hat{E}_i(t + \tau)] \quad (4.5)$$

with a delay τ between the arrivals of signal and idler fields at the BS. Obviously, there is no contribution from first two terms of $|\Psi\rangle$. There are 16 terms in the expansion of Eq. (4.4) when we substitute Eq. (4.5) into Eq. (4.4). Among them ten terms of the form $E_s E_s E_s E_s$, $E_i E_i E_i E_i$, $E_s E_s E_s E_i$, and $E_s E_i E_i E_i$ will give zero result when applied to the state $|\Phi_2\rangle$. The six nonzero terms correspond to the six possibilities in the simple picture of four-photon interference. They are listed as follows:

$$\hat{E}_s(t_1)\hat{E}_s(t_2)\hat{E}_i(t_3 + \tau)\hat{E}_i(t_4 + \tau)|\Psi\rangle,$$

$$\hat{E}_i(t_1 + \tau)\hat{E}_i(t_2 + \tau)\hat{E}_s(t_3)\hat{E}_s(t_4)|\Psi\rangle,$$

$$\hat{E}_s(t_1)\hat{E}_i(t_2 + \tau)\hat{E}_s(t_3)\hat{E}_i(t_4 + \tau)|\Psi\rangle,$$

$$\hat{E}_s(t_1)\hat{E}_i(t_2 + \tau)\hat{E}_i(t_3 + \tau)\hat{E}_s(t_4)|\Psi\rangle,$$

$$\hat{E}_i(t_1 + \tau)\hat{E}_s(t_2)\hat{E}_i(t_3 + \tau)\hat{E}_s(t_4)|\Psi\rangle,$$

$$\hat{E}_i(t_1 + \tau)\hat{E}_s(t_2)\hat{E}_s(t_3)\hat{E}_i(t_4 + \tau)|\Psi\rangle.$$

Since all the six terms are the same except the time variables, we will only present the calculation for the first term with $\tau=0$ and the rest can be obtained by replacing the time variables. By using Eq. (2.1), we have

$$\begin{aligned} & \hat{E}_s(t_1)\hat{E}_s(t_2)\hat{E}_i(t_3)\hat{E}_i(t_4)|\Psi\rangle \\ &= \frac{\eta^2|\text{vac}\rangle}{2(2\pi)^2} \int d\omega_1 d\omega'_1 d\omega_2 d\omega'_2 \Phi(\omega_1, \omega_2)\Phi(\omega'_1, \omega'_2) \\ & \quad \times (e^{-i\omega_1 t_1 - i\omega'_1 t_2} + e^{-i\omega'_1 t_1 - i\omega_1 t_2})(e^{-i\omega_2 t_3 - i\omega'_2 t_4} \\ & \quad + e^{-i\omega'_2 t_3 - i\omega_2 t_4}). \end{aligned} \tag{4.6}$$

By making the exchanges $\omega_1 \leftrightarrow \omega'_1$ or $\omega_2 \leftrightarrow \omega'_2$ in some of the terms in the expansion of the multiplication in the integrand, we find

$$\begin{aligned} & \hat{E}_s(t_1)\hat{E}_s(t_2)\hat{E}_i(t_3)\hat{E}_i(t_4)|\Psi\rangle \\ &= \frac{\eta^2|\text{vac}\rangle}{(2\pi)^2} \int d\omega_1 d\omega'_1 d\omega_2 d\omega'_2 e^{-i\omega_1 t_1 - i\omega'_1 t_2 - i\omega_2 t_3 - i\omega'_2 t_4} \\ & \quad \times [\Phi(\omega_1, \omega_2)\Phi(\omega'_1, \omega'_2) + \Phi(\omega'_1, \omega_2)\Phi(\omega_1, \omega'_2)]. \end{aligned} \tag{4.7}$$

Substitute the above into the six nonzero terms with the appropriate time variables and add them together, we have after some manipulation

$$\begin{aligned} & p_4(t_1, t_2, t_3, t_4) \\ &= \frac{|\eta|^4}{(4\pi)^4} \left| \int d\omega_1 d\omega'_1 d\omega_2 d\omega'_2 e^{-i\omega_1 t_1 - i\omega'_1 t_2 - i\omega_2 t_3 - i\omega'_2 t_4} \right. \\ & \quad \times \{ \Phi(\omega_1, \omega_2)\Phi(\omega'_1, \omega'_2) + \Phi(\omega'_1, \omega_2)\Phi(\omega_1, \omega'_2) \\ & \quad \left. + \bar{\Phi}(\omega_1, \omega'_1)\bar{\Phi}(\omega_2, \omega'_2) \right|^2, \end{aligned} \tag{4.8}$$

where

$$\bar{\Phi}(\omega_1, \omega_2) \equiv \Phi(\omega_1, \omega_2)(e^{i\omega_1 \tau} + e^{i\omega_2 \tau}). \tag{4.9}$$

After integrating over the time variables, we obtain the overall quadruple detection probability

$$\begin{aligned} P_4(\tau) &= \frac{|\eta|^4}{2^4} \int d\omega_1 d\omega'_1 d\omega_2 d\omega'_2 |\Phi(\omega_1, \omega_2)\bar{\Phi}(\omega'_1, \omega'_2) \\ & \quad + \bar{\Phi}(\omega'_1, \omega_2)\bar{\Phi}(\omega_1, \omega'_2) + \bar{\Phi}(\omega_1, \omega'_1)\bar{\Phi}(\omega_2, \omega'_2)|^2. \end{aligned} \tag{4.10}$$

After expanding the absolute value in the integrand, we find

$$\begin{aligned} P_4(\tau) &= \frac{|\eta|^4}{2^4} \int d\omega_1 d\omega'_1 d\omega_2 d\omega'_2 \{ 3|\bar{\Phi}(\omega_1, \omega_2)\bar{\Phi}(\omega'_1, \omega'_2)|^2 \\ & \quad + 6 \text{Re} \bar{\Phi}(\omega_1, \omega_2)\bar{\Phi}(\omega'_1, \omega'_2)\bar{\Phi}^*(\omega'_1, \omega_2) \\ & \quad \times \bar{\Phi}^*(\omega_1, \omega'_2) \}. \end{aligned} \tag{4.11}$$

Here we made exchange of variables in some terms and made use of the symmetry relation $\bar{\Phi}(\omega_1, \omega_2) = \bar{\Phi}(\omega_2, \omega_1)$. After substituting Eq. (4.9) in Eq. (4.11), we have

$$\begin{aligned} P_4(\tau) &= \alpha \{ \mathcal{A}[1 + q(\tau)]^2 \\ & \quad + \mathcal{E} + \text{Re}[2\mathcal{E}_1(\tau) + 2\mathcal{E}_2(\tau) + 2\mathcal{E}_3(\tau) + \mathcal{E}_4(\tau)] \}, \end{aligned} \tag{4.12}$$

where α is some proportional constant, \mathcal{A} and \mathcal{E} are given in Eqs. (2.15) and (2.16),

$$q(\tau) = \frac{\int d\omega_1 d\omega_2 |\Phi(\omega_1, \omega_2)|^2 e^{i(\omega_1 - \omega_2)\tau}}{\int d\omega_1 d\omega_2 |\Phi(\omega_1, \omega_2)|^2}, \tag{4.13}$$

and

$$\mathcal{E}_1(\tau) = \int d\omega_1 d\omega_2 d\omega'_1 d\omega'_2 \Phi(\omega_1, \omega_2)\bar{\Phi}(\omega'_1, \omega'_2)\bar{\Phi}^*(\omega'_1, \omega_2)\bar{\Phi}^*(\omega_1, \omega'_2)e^{i(\omega_2 - \omega_1)\tau}, \tag{4.14}$$

$$\mathcal{E}_2(\tau) = \int d\omega_1 d\omega_2 d\omega'_1 d\omega'_2 \Phi(\omega_1, \omega'_1)\bar{\Phi}(\omega_2, \omega'_2)\bar{\Phi}^*(\omega_1, \omega_2)\bar{\Phi}^*(\omega'_1, \omega'_2)e^{i(\omega_2 - \omega_1)\tau}, \tag{4.15}$$

$$\mathcal{E}_3(\tau) = \int d\omega_1 d\omega_2 d\omega'_1 d\omega'_2 \Phi(\omega_1, \omega'_1)\bar{\Phi}(\omega_2, \omega'_2)\bar{\Phi}^*(\omega_1, \omega'_2)\bar{\Phi}^*(\omega'_1, \omega_2)e^{i(\omega_2 - \omega_1)\tau}, \tag{4.16}$$

$$\mathcal{E}_4(\tau) = \int d\omega_1 d\omega_2 d\omega'_1 d\omega'_2 \Phi(\omega_1, \omega_2)\bar{\Phi}(\omega'_1, \omega'_2)\bar{\Phi}^*(\omega'_1, \omega_2)\bar{\Phi}^*(\omega_1, \omega'_2)e^{i(\omega_2 + \omega'_2 - \omega_1 - \omega'_1)\tau}. \tag{4.17}$$

Here $\mathcal{E}_1^* = \mathcal{E}_2$, $\mathcal{E}_3^* = \mathcal{E}_3$. Notice that $q(0) = 1$, and $\mathcal{E}_{1,2,3,4}(0) = \mathcal{E}$. So we have

$$P_4(0) = \alpha(4\mathcal{A} + 8\mathcal{E}). \tag{4.18}$$

When the delay is zero, maximum interference occurs. This

is the multimode equivalence of the quantum-mechanical case described in Eq. (4.1). On the other hand, if $\Phi(\omega_1, \omega_2)$ has a nonzero bandwidth, then $q(\infty) = 0$, and $\mathcal{E}_{1,2,3,4}(\infty) = 0$. Therefore

$$P_4(\infty) = \alpha(\mathcal{A} + \mathcal{E}). \tag{4.19}$$

When the delay is large, no interference occurs, which corresponds to the classical case. So the ratio

$$\frac{P_4(0)}{P_4(\infty)} = 4 + \frac{4\mathcal{E}}{\mathcal{A} + \mathcal{E}} \quad (4.20)$$

is the multimode result for the quantity P_4^q/P_4^c in Eq. (4.3). In the ideal condition when $\mathcal{E} = \mathcal{A}$, we have

$$\frac{P_4^q}{P_4^c} = 6, \quad (4.21)$$

which is exactly same as in Eq. (4.3) for the single mode case.

V. DISCUSSION AND SUMMARY

We have analyzed four interference schemes involving fields from two independent parametric down-conversion processes. We have shown that the visibilities of interference fringe in these schemes are related to the quantity \mathcal{E}/\mathcal{A} , which is also a measure of photon bunching effect for one field (signal or idler) of parametric down-conversion. Photon bunching can be easily measured experimentally: the access coincidence gives rise to \mathcal{E} while the accidental coincidence corresponds to \mathcal{A} when we measure the autocorrelation of intensity. By identifying the quantity that is responsible for the visibility, we are able to see what influence its value and improve the visibility. By measuring the quantity \mathcal{E}/\mathcal{A} (involving only two-photon coincidence and having higher rate), we can predict what will be the visibility of interference involving four-photon coincidence measurement, which has much lower rate.

The quantity \mathcal{E}/\mathcal{A} only concerns temporal mode matching; the effect of imperfect alignment will influence spatial mode matching. In the above discussion, we have assumed that the spatial modes are perfectly matched so that it is not a factor in visibility. However, the situation can never be ideal experimentally. Spatial mode can be easily incorporated in the discussion above by multiplying the respective spatial factor $\exp(ik_s \cdot x)$ in the integrands of the field operators in Eqs. (2.17) and (3.26) and later taking average of the corresponding position x over the size of the detectors. It can be shown

after some calculation that the effect is simply a modification of all the τ -dependent functions by a factor of $\gamma \equiv (\sin \beta/\beta)^2$ with $\beta = \pi \Delta x/L$. Here Δx is the size of the detectors and L is the interference fringe spacing due to misalignment. For example, $\mathcal{E}(\tau)$ will be replaced by $\gamma \mathcal{E}(\tau)$ in Eq. (3.12) and $q(\tau)$ by $\gamma q(\tau)$ in Eq. (4.12), etc. Then the visibilities are modified as follows: Eq. (3.13) is changed to

$$v = \frac{\gamma \mathcal{E}}{2\mathcal{A} + \mathcal{E}}, \quad (5.1)$$

Eq. (3.20) to

$$v = \gamma \mathcal{E}/\mathcal{A}, \quad (5.2)$$

Eq. (3.37) to

$$v = \frac{\gamma \mathcal{E}}{2\mathcal{A} - \gamma \mathcal{E}}, \quad (5.3)$$

and Eq. (4.20) to

$$\frac{P_4(0)}{P_4(\infty)} = (1 + \gamma)^2 + (5 - \gamma) \frac{\gamma \mathcal{E}}{\mathcal{A} + \mathcal{E}}. \quad (5.4)$$

Since $\gamma \leq 1$, the effect of misalignment is to reduce the interference effect.

Although four-photon state is used here in Sec. IV, the four-photon state cannot be used for a demonstration of GHZ nonlocality because it is in the form of $|2,2\rangle$. The two photons in each mode of $|2,2\rangle$ are indistinguishable and therefore inseparable. To demonstrate GHZ nonlocality, the four photons in the four-photon GHZ state have to be in separate modes, or in other words, they are distinguishable. For the scheme of a recent demonstration [24] of three-photon GHZ state, we can carry out a multimode analysis along the line developed in this paper and show that the visibility is simply \mathcal{E}/\mathcal{A} .

ACKNOWLEDGMENT

Z.Y.O. was supported by the U.S. Office of Naval Research.

-
- [1] D. M. Greenberger, M. A. Horne, and A. Zeilinger, in *Bell's Theorem, Quantum Theory, and Conceptions of the Universe*, edited by M. Kafatos (Kluwer Academic, Dordrecht, The Netherlands, 1989); D. M. Greenberger, M. A. Horne, A. Shimony, and A. Zeilinger, *Am. J. Phys.* **58**, 575 (1990).
- [2] B. Yurke and D. Stoler, *Phys. Rev. Lett.* **68**, 1251 (1992).
- [3] A. Zeilinger, M. A. Horne, H. Weinfurter, and M. Zukowski, *Phys. Rev. Lett.* **78**, 3031 (1997).
- [4] C. H. Bennett, G. Brassard, C. Crepeau, R. Jozsa, A. Peres, and W. K. Wothers, *Phys. Rev. Lett.* **70**, 1895 (1993).
- [5] D. Bouwmeester, J.-W. Pan, K. Mattle, M. Eibl, H. Weinfurter, and A. Zeilinger, *Nature (London)* **390**, 575 (1997).
- [6] M. Zukowski, A. Zeilinger, M. A. Horne, and A. K. Ekert, *Phys. Rev. Lett.* **71**, 4287 (1993).
- [7] J.-W. Pan, D. Bouwmeester, H. Weinfurter, and A. Zeilinger, *Phys. Rev. Lett.* **80**, 3891 (1998).
- [8] P. Shor, *Proceedings of the 35th Symposium on the Foundations of Computer Science* (IEEE Computer Society, Los Alamitos, CA, 1994), pp. 124–134.
- [9] P. G. Kwiat, K. Mattle, H. Weinfurter, A. Zeilinger, A. V. Sergienko, and Y. H. Shih, *Phys. Rev. Lett.* **75**, 4337 (1995).
- [10] Z. Y. Ou, *Phys. Rev. A* **37**, 1607 (1988).
- [11] M. Zukowski, A. Zeilinger, and H. Weinfurter, *Ann. (N.Y.) Acad. Sci.* **755**, 91 (1995).
- [12] J. G. Rarity, *Ann. (N.Y.) Acad. Sci.* **755**, 624 (1995).
- [13] Z. Y. Ou, *Quantum Semiclass. Opt.* **9**, 599 (1997).
- [14] R. Hanbury Brown and R. Q. Twiss, *Nature (London)* **177**, 27 (1956).

- [15] S. Carusotto, Phys. Rev. A **11**, 1629 (1975).
- [16] B. Yurke and M. Potasek, Phys. Rev. A **36**, 3464 (1987).
- [17] A. Zeilinger, M. Zukowski, M. A. Horne, H. J. Bernstein, and D. M. Greenberger, in *Quantum Interferometry*, edited by F. DeMartini and A. Zeilinger (World Scientific, Singapore, 1994); M. Zukowski, A. Zeilinger, and M. A. Horne, Phys. Rev. A **55**, 2564 (1997).
- [18] C. K. Hong and L. Mandel, Phys. Rev. Lett. **56**, 58 (1986).
- [19] C. K. Hong, Z. Y. Ou, and L. Mandel, Phys. Rev. Lett. **59**, 2044 (1987).
- [20] J.-K. Rhee and L. J. Wang (unpublished).
- [21] S. L. Braunstein and A. Mann, Phys. Rev. A **51**, R1727 (1995); **53**, 630(E) (1996).
- [22] M. Pavicic and J. Summhammer, Phys. Rev. Lett. **73**, 3191 (1994).
- [23] R. A. Campos, B. E. A. Saleh, and M. C. Teich, Phys. Rev. A **40**, 1371 (1990).
- [24] D. Bouwmeester, J.-W. Pan, M. Daniell, H. Weinfurter, and A. Zeilinger, Phys. Rev. Lett. **82**, 1345 (1999).